Title Page

Budding of Ebola virus particles requires the Rab11-dependent endocytic recycling pathway

Asuka Nanbo* and Yusuke Ohba

Faculty of Medicine and Graduate School of Medicine, Hokkaido University, Sapporo, Japan.

Word counts: abstract, 191; text, 3071

Footnote Page

A conflict of interest statement

The authors declare that the research was conducted in the absence of any commercial or financial relationships that could be construed as a potential conflict of interest.

A funding statement

This work was supported by grants from Japan Society for the Promotion of Science (23790493), Japan Science and Technology Agency (01-117), Daiichi Sankyo Foundation of Life Science, Hayashi Memorial Foundation for Female Natural Scientists, Mochida Memorial Foundation for Medical and Pharmaceutical Research, Suhara Memorial Foundation, and Akiyama Life Science Foundation to AN. The funders had no role in study design, data collection and analysis, decision to publish or preparation of the manuscript. The authors declare that this work has not previously been presented in any meetings.

* **Corresponding author contact information**

Asuka Nanbo, Ph.D.

Faculty of Medicine and Graduate School of Medicine, Hokkaido University, Kita 15 Nishi 7, Kita-ku, Sapporo, Japan 060-8638

Phone: +81-11-706-5158

Fax: +81-11-706-7877

E-mail : nanboa@med.hokudai.ac.jp

Alternate corresponding author contact information

Yusuke Ohba, MD, Ph.D.

Faculty of Medicine and Graduate School of Medicine, Hokkaido University, Kita 15 Nishi 7, Kita-ku, Sapporo, Japan 060-8638

Phone: +81-11-706-5158

Fax: +81-11-706-7877

E-mail : yohba@med.hokudai.ac.jp

Abstract

The Ebola virus-encoded major matrix protein VP40 traffics to the plasma membrane, which leads to the formation of filamentous viral particles and subsequent viral egress. However, the cellular machineries underlying this process are not fully understood. In the present study, we have assessed the role of host endocytic recycling in Ebola virus particle formation. We found that a small GTPase Rab11, which regulates recycling of molecules between the trans-Golgi network, recycling endosomes, and the plasma membrane, was incorporated in Ebolavirus-like particles. While Rab11 predominantly localized in the perinuclear region, it distributed diffusely in the cytoplasm and partly localized in the periphery of the cells transiently expressing VP40. In contrast, Rab11 exhibited a perinuclear distribution when two VP40 derivatives that lack ability to traffic to the plasma membrane were expressed. Finally, expression of a dominant-negative form of Rab11 or knockdown of Rab11 inhibited both VP40-induced clusters at the plasma membrane and release of viral-like particles. Taken together, our findings demonstrate that Ebola virus exploits host endocytic recycling machinery to facilitate the trafficking of VP40 to the cell

surface and the subsequent release of viral-like particles for its establishment of efficient viral egress.

Keywords: Ebola virus, VP40, virus egress, viral-like particles, Rab11, recycling endosome

Introduction

Ebola virus (EBOV), a member of the family *Filoviridae*, is an enveloped, single-stranded, negative-sense RNA virus that causes severe hemorrhagic fever with a high mortality rate in humans and nonhuman primates [1]. Currently, there are no FDA-approved therapeutics to treat EBOV infection [2]. Ebola virus encodes seven structural genes that assemble to yield distinct filamentous viral particles. The EBOV-encoded major matrix protein VP40 traffics to the plasma membrane (PM), which leads to the formation and release of the virus-like particles (VLPs), even when expressed alone [3-7]. VP40 has been shown to form a dimer which further assembles into a flexible filamentous matrix structure [8].

VP40 contains two overlapping late domains (PTAP and PPXY motifs) that interact with Tsg101, a component of the endosomal sorting complex required for transport (ESCRT)-1, and with the ubiquitin ligase Nedd4, respectively [9]. Although both late domains are responsible for release of VLPs [10, 11], a study using recombinant EBOV showed that the late domains are dispensable for virus replication [12]. It has been shown

91 that several host factors are required for the intracellular transport of VP40, including actin
92 [13-15], IQGAP1, a ubiquitously expressed scaffolding protein that regulates processes that
93 include cell motility and division, actin polymerization, and formation of filopodia [16],
94 Sec24C, a component of the host COPII vesicular transport system [17], microtubules [18],
95 and the HECT family E3 ubiquitin ligase WWP1 [19]. However, the molecular mechanisms
96 of VP40-mediated Ebola virus egress have not been fully elucidated.

97 The host endocytic recycling machinery and its major regulator, a small GTPase
98 Ras-related in brain (Rab) 11, are implicated in the virus lifecycle including assembly and
99 viral egress [20]. Rab11 associates with recycling endosomes and regulates recycling
100 processes of proteins and vesicles to the cell surface [21]. Rab11 also localizes to the
101 trans-Golgi network (TGN) and post-Golgi vesicles, and has been implicated in the
102 trafficking between the TGN and the endosomal recycling compartments through the
103 regulated secretion pathway [22].

104 The Rab11-dependent recycling pathway involves trafficking of virus
105 components to their sites of egress. It has been shown that Rab11-positive vesicles

106 associate with viral ribonucleoproteins (vRNPs) of a variety of viruses, including influenza
107 A virus (IAV) [23-26], Sendai virus [27, 28], and human parainfluenza virus type I [28],
108 and promote their trafficking toward their sites of egress. Herpes simplex virus-1 exploits
109 the same pathway to transport its viral glycoproteins on the PM to the intracellular
110 compartment for maturation of virions [29]. The Nipah virus-encoded fusion protein is
111 activated by cleavage with cathepsin B in the recycling endosomes, and subsequently
112 recycled to the PM for incorporation in the virions [30]. The accessory protein Vpu of
113 human immunodeficiency virus 1 is transported via Rab11-positive vesicles toward the
114 assembly site on the PM [31].

115 Moreover, a potential role for the Rab11-dependent endocytic recycling pathway
116 in viral egress has been suggested for both positive- and negative-sense RNA viruses. The
117 Rab11-dependent pathway involves budding of respiratory syncytial virus (RSV) [32, 33]
118 and the filamentous IAV [34] by facilitating fission of viral particles from the PM. The
119 Rab11-mediated pathway is also implicated in egress from the PM for Mason-Pfizer
120 monkey virus [35, 36], Jaagsiekte sheep retrovirus [37], and hepatitis C virus [38], which

121 are originally assembled and mature respectively at the microtubule organizing center, the
122 endoplasmic reticulum, and the Golgi/TGN compartments.

123 Although a previous study using liquid chromatography-linked tandem mass
124 spectroscopy (LC-MS/MS) showed that Rab11b is incorporated into authentic filovirus
125 virions [39], its physiological relevance in the EBOV lifecycle has remained unclear. In the
126 present study, we have assessed the role of the Rab11-dependent recycling pathway in
127 VP40-mediated budding of Ebola virus-like particles (VLPs). We found that Rab11 was
128 incorporated into Ebola VLPs. While Rab11 predominantly localized in the perinuclear
129 region, it distributed diffusely in the cytoplasm and partly localized in the periphery of the
130 cells transiently expressing VP40. Blocking of endosomal recycling by the expression of a
131 dominant-negative form of Rab11 or by knockdown of endogenous Rab11 suppressed the
132 VP40-induced formation of clusters at the PM. Moreover, downregulation of Rab11
133 reduced the production of Ebola VLPs. Taken together, our findings indicate that EBOV
134 exploits host endocytic recycling machinery for its establishment of efficient viral egress.
135

Materials and Methods

Cell culture

African green monkey kidney epithelial Vero-E6 cells and human embryonic kidney HEK293T cells (American Type Culture Collection) were grown in high-glucose Dulbecco's modified Eagle's medium (DMEM) containing 10% fetal bovine serum (FBS) and antibiotics. Cells were maintained at 37°C in 5% CO_2. Transfection of Vero-E6 and HEK293T cells with expression plasmids and small interference RNA (siRNA) was carried out with TransIT-LT1 (Mirus, Madison, WI) and TransIT-TKO (Mirus), respectively.

Plasmids

The expression plasmids of EBOV VP40 L117R and I307R mutants were constructed by insertion into the pCAGGS plasmid at the EcoRI and BglII sites. VP40 mutant cDNAs were amplified by PCR using the following oligonucleotides: VP40-L117R, Forward 5'-actacggccgccatcatgcgtgcttcatac-3' and Reverse 5'-gggtgatagtgtatgaagcacgcatgatgg-3', VP40-I307R, Forward

5’-ggagacctcaccatggtaagaacacaggatt-3’ and Reverse 5’-acgtgtcacaatcctgtgttcttaccatggt-3’. The pEGFP-C3 plasmids encoding green fluorescent protein (GFP)-fused wild-type Rab11 (GFP-wtRab11) and a dominant-negative form of Rab11 (GFP-dnRab1) were kind gifts from Dr. Angela Wandinger-Ness (University of New Mexico) [40].

Preparation of Ebola virus-like particles (Ebola VLPs)

The preparation of Ebola VLPs was described previously [41, 42]. Briefly, equal amounts of the pCAGGS expression plasmids for EBOV subtype Zaire, strain Mayinga VP40, GP, and NP were transfected into HEK293T cells. Forty-eight hours post-transfection (h.p.t.), the culture supernatants were harvested, and centrifuged at 1,500 rpm for 5 min and then at 3,500 rpm for 15 min to remove detached cells and cell debris, respectively. The VLPs were pelleted through a 30% sucrose cushion by centrifugation at 11,000 rpm for 1 h at 4°C with an SW40 rotor (Beckman, Fullerton, USA). The pelleted VLPs were resuspended in PBS. For a protease protection assay, Ebola VLPs were treated with or without 0.1 mg/ml trypsin in the presence or absence of 0.05% Triton X-100 at

166 room temperature for 30 min, followed by the addition of SDS-PAGE sample buffer. The
167 incorporation of VP40 and Rab11 in the purified VLPs was confirmed by western blotting
168 with the mouse monoclonal antibodies against VP40 (clone 6; 1:4000 dilution) and Rab11
169 (Becton, Dickinson and Company, Franklin Lakes, NJ, USA; 1:1000 dilution), respectively.
170 The experiment was performed three times independently and the intensity of the bands
171 was quantified by use of Multigauge software (Fujifilm corporation).
172
173 **Immunofluorescence staining**
174 Vero-E6 cells grown on coverslips were transfected with the expression plasmid for VP40,
175 VP40-L117R, or VP40-I307R. At 48 h.p.t., the cells were fixed with 4% paraformaldehyde
176 in PBS for 10 min at room temperature, permeabilized with PBS containing 0.05% Triton
177 X-100 for 10 min at room temperature and blocked in PBS containing 4% BSA for 20 min
178 at room temperature. The cells were then incubated with a mouse monoclonal antibody
179 against VP40 (clone 6; 1:2000 dilution), or a rabbit polyclonal antibody against Rab11
180 (Abcam, Cambridge, UK; 1:200 dilution) for 1 h at room temperature. The cells were then

181 washed three times in PBS and incubated with Alexa Fluor 488 or 594-labeled secondary
182 antibodies (Thermo Fisher Scientific, Waltham, USA; 1:2000 dilution) for 1 h at room
183 temperature After washing, nuclei were counterstained with Hoechst 33342 (Cell Signaling
184 Technology, Trask Lane, USA). To determine the effect of expression of GFP-wtRab11 or
185 -dnRab11 on the distribution of VP40, Vero-E6 cells were transfected with pEGFP-C3
186 plasmids encoding GFP-wtRab11 or -dnRab11. Forty-eight hours later, the cells were
187 transfected with the expression plasmid for VP40. At 48 h.p.t., the cells were harvested
188 followed by immunofluorescence staining with the antibody for VP40. Images were
189 collected with the 60 × oil-immersion objective lens of a confocal laser scanning
190 microscope (Fluoview FV10i, Olympus, Tokyo, Japan) and acquired by using FV10-ASW
191 software (Olympus). Line scan imaging was performed by using FV10-ASW software.
192
193 **siRNA treatment**
194 Target sequences corresponding to the human Rab11a and Rab11b-coding
195 sequences were selected and synthesized (Life Technologies) [43]. As a control, a siRNA

196 encoding a sequence that does not target any known genes (Thermo Fisher Scientific) was
197 used. siRNAs against Rab11a and/or Rab11b were transfected into Vero-E6 or HEK293T
198 cells. At 72 h.p.t, the downregulation of Rab11 in Vero-E6 and HEK293T cells was
199 analyzed by immunofluorescence staining and western blotting with a mouse anti-Rab11
200 monoclonal antibody (Becton, Dickinson and Company), a rabbit anti-Rab11 polyclonal
201 antibody (Abcam), and a rabbit anti-β-actin polyclonal antibody (MBL), respectively. For
202 the analysis of the effect of downregulation of Rab11 on distribution of VP40,
203 siRNA-transfected Vero-E6 cells were then transfected with the expression plasmid of
204 VP40 at 72 h.p.t., followed by immunofluorescence staining by means of a mouse
205 monoclonal antibody for VP40. For the analysis of the effect of downregulation of Rab11
206 on production of Ebola VLPs, siRNA-transfected HEK293T cells were then transfected
207 with the expression plasmids of VP40, NP, and GP at 72 h.p.t., followed by purification of
208 Ebola VLPs as described above. Expression of EBOV proteins in the total cell lysates and
209 the purified VLPs was confirmed by western blotting with the mouse monoclonal
210 antibodies against VP40 (clone 6; 1:4000 dilution), NP (clone 7.42.18; 1:4000 dilution), or

GP (clone 133.13.16.; 1:4000 dilution), respectively. The experiment was performed three times independently and the intensity of the bands was quantified by use of Multigauge software.

Results

Rab11 is incorporated into Ebola VLPs.

In the present study, we first examined whether Rab11 is incorporated into Ebola VLPs by a protease protection assay [5]. We generated Ebola VLPs by co-expressing VP40, GP, and NP in HEK293T cells [41, 42]. Ebola VLPs were treated with or without trypsin in the presence or absence of Triton X-100 at room temperature for 30 min followed by western blot analysis. While both VP40 and Rab11 was detected in Ebola VLPs treated with trypsin or Triton X-100 alone, trypsinization in the presence of Triton X-100 significantly abolished the signals of VP40 and Rab11 (Figure 1), indicating the incorporation of Rab11 in Ebola VLPs.

VP40 induces a dispersed distribution of Rab11.

We then investigated the subcellular localization of Rab11 in Vero-E6 cells transiently expressing the EBOV VP40 by immunofluorescence staining. Rab11 predominantly distributed in perinuclear regions and some fraction of the protein distributed in the cytoplasm in backbone plasmid-transfected control cells (Figure 2A), which is consistent with a prior study [40] showing its localization to recycling endosomes and TGN. In agreement with previous findings [4, 5, 44-46], VP40 distributed in multiple subcellular compartments (Figure 2B). VP40 was visualized diffusely in the cytoplasm and the nucleus, and particularly in the PM as intense clusters. In contrast, co-immunofluorescence staining revealed the disperse distribution of Rab11 throughout the cytoplasm in the cells expressing high level of VP40 (Figure 2B, insets a and b). However, no efficient colocalization of Rab11 along with VP40 was observed.

We also analyzed the distribution of Rab11 in cells transiently expressing two types of VP40 derivatives, L117R (Figure 2C) and I370R (Figure 2D), which lack the ability to traffic to the PM and subsequent VLP formation [8]. In agreement with previous findings,

241 both mutants remained in the cytoplasm and failed to form clusters at the PM. Rab11
242 distributed in the perinuclear region of cells expressing both VP40 mutants, suggesting its
243 dispersed distribution is likely associated with trafficking of VP40 to the PM.
244
245 **The effect of a dominant-negative form of Rab11 on distribution of VP40.**
246 Because the distribution of Rab11 was affected by VP40 (Figure 2), we
247 investigated the role of Rab11 in VP40-induced viral particle formation. We transfected
248 Vero-E6 cells and transiently expressed both GFP-fused wild-type (GFP-wtRab11) or a
249 dominant-negative form of Rab11 (GFP-dnRab11), which has an amino acid substitution
250 (S25N) [40], and expression plasmids for VP40. We then assessed the effect of Rab11
251 derivatives on the distribution of VP40 by immunofluorescence staining. When
252 GFP-wtRab11 was expressed alone, it exhibited a predominant distribution in the
253 perinuclear region in the same way as does endogenous Rab11 (Figure 2A v.s. Figure 3A).
254 In contrast, GFP-wtRab11 was predominantly distributed diffusely throughout the
255 cytoplasm in VP40-positive cells (Figure 3B). VP40 distributed in the periphery of the cells

256 expressing GFP-wtRab11 with intense clusters (Figure 3B). GFP-dnRab11 predominantly
257 distributed in the cytoplasm in both VP40-negative and -positive cells (Figure 3C and 3D).
258 In the presence of GFP-dnRab11 expression, VP40 distributed in the cytoplasm without
259 formation of clusters in the PM, suggesting that the expression of GFP-dnRab11 suppressed
260 formation of VP40-induced clusters in the PM (Figure 3D). GFP-wtRab11 and -dnRab11
261 were partly distributed in the PM of the cells expressing VP40 (Figure 3B and 3D).
262 However, efficient colocalization of Rab11 derivatives with VP40 was not observed, which
263 is consistent with the result in Figure 2B.
264
265 **A Rab11-dependent endocytic recycling pathway contributes to VP40-mediated Ebola**
266 **VLP formation.**
267 We further assessed the role of Rab11 in VP40-mediated viral particle formation
268 by knockdown of endogenous Rab11 isoforms by means of small interference RNAs
269 (siRNA). Rab11 consists of three isoforms Rab11a, Rab11b, and Rab25. Rab11a and
270 Rab11b share 90% amino acid sequence identity, whereas Rab11a and Rab11b share about

60% identity with Rab25. Rab11a is expressed ubiquitously, predominantly localizes to recycling endosomes, and functions in the recycling of a wide range of molecules to the cell surface [22]. Rab11b is expressed in the heart, brain and testes and functions in recycling of molecules in polarized cells [47]. Rab25 has been shown to contribute to the invasiveness of cancer cells by promoting integrin trafficking [48]. Multiple studies have demonstrated that Rab11a functions in the lifecycle of a variety of viruses [20]. Moreover, LC-MS/MS has demonstrated the incorporation of Rab11b into authentic filovirus virions [39]. Thus, we assessed the effect of downregulation of Rab11a and Rab11b isoforms in VP40-mediated formation of Ebola VLPs. We transfected HEK293T cells with siRNAs for Rab11a and/or Rab11b isoforms. At 72 h.p.t, expression plasmids for VP40, NP and GP were transfected to produce VLPs. We confirmed that knockdown of Rab11 isoforms minimally affected the expression of VP40 (Figure 4A). We found that the downregulation of both Rab11a alone and of both its isoforms significantly suppressed the formation of Ebola VLPs (Figure 4B), indicating that Rab11 plays a crucial role in the budding of Ebola viral particles.

We further examined the effect of Rab11 knockdown on the distribution of VP40 in Vero-E6 cells. The cells in which Rab11a and b isoforms were downregulated suppressed the formation of VP40-positive clusters at the PM (Figure 5B), which was observed in control siRNAs-treated cells (Figure 5A). Remaining clusters on the PM (white arrows) are likely derived from the incomplete knockdown of Rab11 (Figure 4A). The data indicates that the cluster formation of VP40 to the PM and the subsequent VLP formation require Rab11-dependent endocytic recycling pathway.

Discussion

It has been shown that Rab11 is pivotal for both assembly and egress of various viruses [9]. Here, we demonstrate that Rab11 plays an important role in trafficking of VP40 to the PM and the subsequent budding of Ebola VLPs.

Rab11 is a multifunctional molecule that is involved in the endocytic recycling pathway, as well as actin remodeling, cytokinesis, and abscission. Rab11's diverse functions are regulated by interactions with Rab11 family interacting proteins (Rab11-FIPs),

301 which direct Rab11 to specific subcellular locations by binding to actin- or
302 microtubules-associated motor proteins [49].

303 We demonstrated that Rab11 distributed more diffusely in the cytoplasm upon
304 expression of VP40 (Figure 2B) and was subsequently incorporated into Ebola VLPs
305 (Figure 1). We also observed that blocking Rab11 function by expression of a
306 dominant-negative form of Rab11 (Figure 3) and downregulation of Rab11 by siRNAs
307 (Figure 5) abrogated the formation of VP40-induced clusters at the periphery of the cells.

308 These data indicate that VP40 induced an alteration in Rab11-mediated vesicular
309 trafficking toward the PM. Moreover, two types of VP40 derivatives, which lack the ability
310 to transport to the PM and subsequent VLP formation, failed to induce the dispersed
311 distribution of Rab11 (Figure 2C and 2D), suggesting that trafficking of VP40 to the PM is
312 likely associated with the Rab11-dependent trafficking machinery.

313 The Rab11-mediated recycling pathway involves budding of RSV [32, 33] and
314 filamentous IAV virions [34]. For these viruses, Rab11 appears to promote remodeling of
315 membrane morphology, which leads to the scission needed to release particles from the cell

316 surface. The Rab11 effectors proteins FIP1 and FIP2 have been found to facilitate fission of
317 RSV from the apical cell surface. In particular, FIP2 controls the length of the filamentous
318 RSV virions [33]. Moreover, Rab11-FIP3 has been shown to be involved in membrane
319 scission to release filamentous IAV virions from the PM. Rab11-FIP2 is known to recruit
320 the myosin Vb (MyoVb) motor protein for the tethering of recycling endosomes to actin at
321 the microtubule-actin junction, and coordinate delivery to the PM [50]. Rab11-FIP3
322 interacts with the actin-regulating protein Arf6 at the PM [51]. Thus, it is most likely that
323 these Rab11 effector proteins mediate the remodeling the actin cytoskeleton at the PM,
324 which is responsible for the budding of these viruses.

325 Although our data indicates that siRNA treatment for Rab11 suppressed the
326 formation of VP40-positive clusters in the PM (Figure 5) and the production of Ebola VLPs
327 (Figure 4), it is still unclear whether the Rab11-mediated recycling pathway is directly
328 responsible for the cluster formation of VP40 in the PM and/or budding of Ebola VLPs
329 from the cell surface. Moreover, immunofluorescent staining analysis revealed that efficient
330 colocalization of VP40 with endogenous Rab11 and GFP-wtRab11 was not observed

(Figures 2 and 3). Further ultrastructural analyses of the morphology of budding VLPs on the cell surface upon blocking Rab11 function will be required to clarify the role of Rab11 in the process of Ebola VLPs formation. In parallel, characterization of the Rab11-associtated effector proteins underlying this process is needed to better understand the detailed molecular mechanism by which Rab11 contributes to the intracellular trafficking of VP40 and formation of Ebola VLPs.

In summary, our findings indicate that the Rab11-dependent endocytic pathway mediates both trafficking of VP40 to the cell surface and efficient Ebola virus egress.

Acknowledgement

We thank to Dr. Angela Wandinger-Ness (University of New Mexico) for providing the pEGFP-C3 plasmids encoding GFP-fused Rab11 derivatives. We thank to Dr. Bill Sugden for critical reviewing of this manuscript. This work was supported by grants from Japan Society for the Promotion of Science (23790493), Japan Science and Technology Agency (01-117), Daiichi Sankyo Foundation of Life Science, Hayashi Memorial

Foundation for Female Natural Scientists, Mochida Memorial Foundation for Medical and Pharmaceutical Research, Suhara Memorial Foundation, and Akiyama Life Science Foundation to AN. The authors declare that the research was conducted in the absence of any commercial or financial relationships that could be construed as a potential conflict of interest.

References

1. Feldmann H, Sanchez A, Geisbert T. Filoviridae: Marburg and Ebola viruses. In M Knipe and P M Howley (ed), Fields virology, 6th ed Lippincott Williams & Wilkins, Philadelphia, PA **2013**.

2. Wong G, Kobinger GP. Backs against the wall: novel and existing strategies used during the 2014-2015 Ebola virus outbreak. Clin Microbiol Rev **2015**; 28:593-601.

3. Kolesnikova L, Bamberg S, Berghofer B, Becker S. The matrix protein of Marburg virus is transported to the plasma membrane along cellular membranes: exploiting the retrograde late endosomal pathway. J Virol **2004**; 78:2382-93.

4. Hoenen T, Biedenkopf N, Zielecki F, et al. Oligomerization of Ebola virus VP40 is essential for particle morphogenesis and regulation of viral transcription. J Virol **2010**

; 84:7053-63.

5. Jasenosky LD, Neumann G, Lukashevich I, Kawaoka Y. Ebola virus VP40-induced particle formation and association with the lipid bilayer. J Virol **2001**; 75:5205-14.

6. Noda T, Watanabe S, Sagara H, Kawaoka Y. Mapping of the VP40-binding regions of the nucleoprotein of Ebola virus. J Virol **2007**; 81:3554-62.

7. Timmins J, Scianimanico S, Schoehn G, Weissenhorn W. Vesicular release of ebola virus matrix protein VP40. Virology **2001**; 283:1-6.

8. Bornholdt ZA, Noda T, Abelson DM, et al. Structural rearrangement of ebola virus VP40 begets multiple functions in the virus life cycle. Cell **2013**; 154:763-74.

9. Votteler J, Sundquist WI. Virus budding and the ESCRT pathway. Cell Host Microbe **2013**; 14:232-41.

10. Harty RN, Brown ME, Wang G, Huibregtse J, Hayes FP. A PPxY motif within the VP40 protein of Ebola virus interacts physically and functionally with a ubiquitin ligase: implications for filovirus budding. Proc Natl Acad Sci U S A **2000**; 97:13871-6.

11. Yasuda J, Nakao M, Kawaoka Y, Shida H. Nedd4 regulates egress of Ebola virus-like particles from host cells. J Virol **2003**; 77:9987-92.

12. Neumann G, Ebihara H, Takada A, et al. Ebola virus VP40 late domains are not essential for viral replication in cell culture. J Virol **2005**; 79:10300-7.

13. Adu-Gyamfi E, Digman MA, Gratton E, Stahelin RV. Investigation of Ebola VP40 assembly and oligomerization in live cells using number and brightness analysis. Biophys J **2012**; 102:2517-25.

14. Han Z, Harty RN. Packaging of actin into Ebola virus VLPs. Virol J **2005**; 2:92.

15. Kolesnikova L, Ryabchikova E, Shestopalov A, Becker S. Basolateral budding of Marburg virus: VP40 retargets viral glycoprotein GP to the basolateral surface. J Infect Dis **2007**; 196 Suppl 2:S232-6.

16. Liu Y, Cocka L, Okumura A, Zhang YA, Sunyer JO, Harty RN. Conserved motifs within Ebola and Marburg virus VP40 proteins are important for stability, localization, and subsequent budding of virus-like particles. J Virol **2010**; 84:2294-303.

17. Yamayoshi S, Noda T, Ebihara H, et al. Ebola virus matrix protein VP40 uses the COPII transport system for its intracellular transport. Cell Host Microbe **2008**; 3:168-77.

18. Noda T, Ebihara H, Muramoto Y, et al. Assembly and budding of Ebolavirus. PLoS Pathog **2006**; 2:e99.

19. Han Z, Sagum CA, Takizawa F, et al. Ubiquitin Ligase WWP1 Interacts with Ebola Virus VP40 To Regulate Egress. J Virol **2017**; 91.

20. Vale-Costa S, Amorim MJ. Recycling Endosomes and Viral Infection. Viruses **2016**; 8:64.

21. Maxfield FR, McGraw TE. Endocytic recycling. Nat Rev Mol Cell Biol **2004**; 5:121-32.

22. Gromov PS, Celis JE, Hansen C, Tommerup N, Gromova I, Madsen P. Human rab11a: transcription, chromosome mapping and effect on the expression levels of host GTP-binding proteins. FEBS Lett **1998**; 429:359-64.

23. Amorim MJ, Bruce EA, Read EK, et al. A Rab11- and microtubule-dependent mechanism for cytoplasmic transport of influenza A virus viral RNA. J Virol **2011**; 85:4143-56.

24. Avilov SV, Moisy D, Munier S, Schraidt O, Naffakh N, Cusack S. Replication-competent influenza A virus that encodes a split-green fluorescent protein-tagged PB2 polymerase subunit allows live-cell imaging of the virus life cycle. J Virol **2012**; 86:1433-48.

25. Eisfeld AJ, Kawakami E, Watanabe T, Neumann G, Kawaoka Y. RAB11A is essential for transport of the influenza virus genome to the plasma membrane. J Virol **2011**; 85:6117-26.

26. Momose F, Sekimoto T, Ohkura T, et al. Apical transport of influenza A virus ribonucleoprotein requires Rab11-positive recycling endosome. PLoS One **2011**; 6:e21123.

27. Chambers R, Takimoto T. Trafficking of Sendai virus nucleocapsids is mediated by intracellular vesicles. PLoS One **2010**; 5:e10994.

28. Stone R, Hayashi T, Bajimaya S, Hodges E, Takimoto T. Critical role of Rab11a-mediated recycling endosomes in the assembly of type I parainfluenza viruses. Virology **2016**; 487:11-8.

29. Hollinshead M, Johns HL, Sayers CL, Gonzalez-Lopez C, Smith GL, Elliott G. Endocytic tubules regulated by Rab GTPases 5 and 11 are used for envelopment of herpes simplex virus. EMBO J **2012**; 31:4204-20.

30. Diederich S, Sauerhering L, Weis M, et al. Activation of the Nipah virus fusion protein in MDCK cells is mediated by cathepsin B within the endosome-recycling compartment. J Virol **2012**; 86:3736-45.

31. Varthakavi V, Smith RM, Martin KL, et al. The pericentriolar recycling endosome plays a key role in Vpu-mediated enhancement of HIV-1 particle release. Traffic **2006**; 7:298-307.

32. Brock SC, Goldenring JR, Crowe JE, Jr. Apical recycling systems regulate directional budding of respiratory syncytial virus from polarized epithelial cells. Proc Natl Acad Sci U S A **2003**; 100:15143-8.

33. Utley TJ, Ducharme NA, Varthakavi V, et al. Respiratory syncytial virus uses a Vps4-independent budding mechanism controlled by Rab11-FIP2. Proc Natl Acad Sci U S A **2008**; 105:10209-14.

34. Bruce EA, Digard P, Stuart AD. The Rab11 pathway is required for influenza A virus budding and filament formation. J Virol **2010**; 84:5848-59.

35. Pereira LE, Clark J, Grznarova P, et al. Direct evidence for intracellular anterograde co-transport of M-PMV Gag and Env on microtubules. Virology **2014**; 449:109-19.

36. Sfakianos JN, LaCasse RA, Hunter E. The M-PMV cytoplasmic targeting-retention signal directs nascent Gag polypeptides to a pericentriolar region of the cell. Traffic **2003**; 4:660-70.

37. Arnaud F, Murcia PR, Palmarini M. Mechanisms of late restriction induced by an endogenous retrovirus. J Virol **2007**; 81:11441-51.

38. Coller KE, Heaton NS, Berger KL, Cooper JD, Saunders JL, Randall G. Molecular determinants and dynamics of hepatitis C virus secretion. PLoS Pathog **2012**; 8:e1002466.

39. Spurgers KB, Alefantis T, Peyser BD, et al. Identification of essential filovirion-associated host factors by serial proteomic analysis and RNAi screen. Mol Cell Proteomics **2010**; 9:2690-703.

40. Chen W, Feng Y, Chen D, Wandinger-Ness A. Rab11 is required for trans-golgi network-to-plasma membrane transport and a preferential target for GDP dissociation inhibitor. Mol Biol Cell **1998**; 9:3241-57.

41. Nanbo A, Imai M, Watanabe S, et al. Ebolavirus is internalized into host cells via macropinocytosis in a viral glycoprotein-dependent manner. PLoS Pathog **2010**; 6:e1001121.

42. Nanbo A, Maruyama J, Imai M, et al. Ebola virus requires a host scramblase for externalization of phosphatidylserine on the surface of viral particles. PLoS Pathog **2018**; 14:e1006848.

43. Nanbo A, Kachi K, Yoshiyama H, Ohba Y. Epstein-Barr virus exploits host endocytic machinery for cell-to-cell viral transmission rather than a virological synapse. J Gen Virol **2016**; 97:2989-3006.

44. Nanbo A, Watanabe S, Halfmann P, Kawaoka Y. The spatio-temporal distribution dynamics of Ebola virus proteins and RNA in infected cells. Sci Rep **2013**; 3:1206.

45. Watanabe S, Watanabe T, Noda T, et al. Production of novel ebola virus-like particles from cDNAs: an alternative to ebola virus generation by reverse genetics. J Virol **2004**; 78:999-1005.

46. Yamayoshi S, Kawaoka Y. Mapping of a region of Ebola virus VP40 that is important in the production of virus-like particles. J Infect Dis **2007**; 196 Suppl 2:S291-5.

47. Silvis MR, Bertrand CA, Ameen N, et al. Rab11b regulates the apical recycling of the cystic fibrosis transmembrane conductance regulator in polarized intestinal epithelial cells. Mol Biol Cell **2009**; 20:2337-50.

48. Dozynkiewicz MA, Jamieson NB, Macpherson I, et al. Rab25 and CLIC3 collaborate to promote integrin recycling from late endosomes/lysosomes and drive cancer progression. Dev Cell **2012**; 22:131-45.

485 49. Horgan CP, McCaffrey MW. The dynamic Rab11-FIPs. Biochem Soc Trans **2009**;
486 37:1032-6.

487 50. Desnos C, Huet S, Darchen F. 'Should I stay or should I go?': myosin V function in
488 organelle trafficking. Biol Cell **2007**; 99:411-23.

489 51. Donaldson JG. Multiple roles for Arf6: sorting, structuring, and signaling at the plasma
490 membrane. J Biol Chem **2003**; 278:41573-6.

491

492

493

494

495

496

497

498

499

500

501

502

503 **Figure legends**

504 **Figure 1. Rab11 is incorporated into Ebola VLPs.**

505 Characterization of incorporation of Rab11 in Ebola VLPs. HEK293T cells were
506 transfected with expression plasmids for EBOV VP40, GP, and NP. At 48 h.p.t., culture
507 medium was harvested. Viral particles were purified from the culture medium and treated
508 with or without trypsin in the presence or absence of Triton X-100. Incorporation of VP40
509 and Rab11 in Ebola VLPs was analyzed by western blot analysis. The experiment was
510 performed three times independently and representative blot is shown (A). The intensity of
511 the bands was quantified, and the average of the relative expression values and its SD are
512 shown (B). *, $P < 0.05$; **, $P < 0.01$ vs respective control (Student's t-test).

513

514 **Figure 2. Subcellular distribution of Rab11 in the cells transiently expressing VP40**
515 **derivatives.**

516 The subcellular distribution of Rab11 in Vero-E6 cells transiently expressing VP40
517 derivatives. Vero-E6 cells grown on cover slips were transfected with the expression

plasmids for wild-type VP40 (B), VP40 L117R (C), or VP40 I370R (D). At 48 h.p.t., the cells were harvested and the subcellular distribution of VP40 and Rab11 was analyzed by immunofluorescence staining. As a control, a backbone plasmid was transfected (A). In merged images, VP40 and Rab11 are shown in green and magenta, respectively. The nuclei (blue) were counterstained with Hoechst 33342. Insets show the boxed areas. Scale bars: 10 μm.

Figure 3. The effect of a dominant-negative form of Rab11 on the distribution of VP40.

The effect of a dominant-negative form of Rab11 on the distribution of VP40. Vero-E6 cells grown on cover slips were transfected with the expression plasmids for GFP-wtRab11 (B) or -dnRab11 (D). At 48 h.p.t., the cells were transfected with the expression plasmids for VP40. At 48 h.p.t., the cells were harvested and the subcellular distribution of VP40 was analyzed by immunofluorescence staining. As a control, GFP-wtRab11 (A) or -dnRab11 (C) was expressed alone. In merged images, VP40 and GFP-fused Rab11 derivatives are shown in magenta and green, respectively. The nuclei (blue) were counterstained with Hoechst 33342. Scale bars: 10 μm. The plots indicate the individual fluorescence intensity

along each of the corresponding lines. A.U.; arbitrary unit.

Figure 4. Role of Rab11 in budding of Ebola VLPs.

The role of Rab11 in budding of Ebola VLPs. HEK293T cells were transfected with siRNAs against Rab11a, Rab11b alone, or Rab11a and Rab11b. At 72 h.p.t., the cells were transfected with the expression plasmids for VP40, NP and GP. At 48 h.p.t., the cells and culture medium were harvested. Viral particles were purified from the culture medium. Total cell lysates (TCL) (A) and VLPs (B) were analyzed by western blotting with the antibodies against VP40, NP, GP, Rab11, or β-actin. The experiment was performed three times independently and representative blot is shown. The intensity of the bands correspondence to each protein was quantified. The intensity of corresponding bands to VP40, NP, GP, or Rab11 was normalized with that of corresponding bands to β-actin in the same sample. The average of relative expression values and its SD are shown. *, $P < 0.05$; **, $P < 0.01$ vs respective control (Student's t-test).

Figure 5. VP40-induced cluster is formed in a Rab11-dependent manner.

The role of Rab11 in VP40-induced clusters in the PM. Vero-E6 cells were transfected with control siRNAs (A) or siRNAs against Rab11a and Rab11b (B). At 72 h.p.t., the cells were transfected with the expression plasmid of VP40. At 48 h.p.t., the subcellular distribution of VP40 and Rab11 was analyzed by immunofluorescence staining. In merged images, VP40 and Rab11 are shown in green and magenta, respectively. The nuclei (blue) were counterstained with Hoechst 33342. White arrows represent the remaining VP40 clusters in the PM. Scale bars: 10 μm.

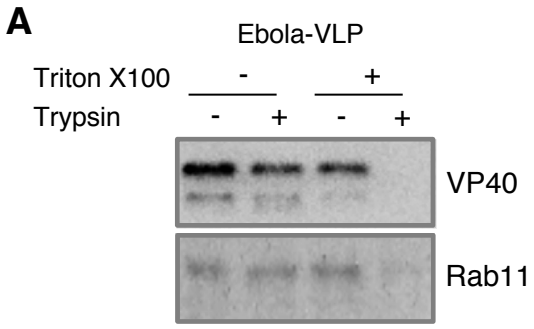
A
Ebola-VLP
Triton X100
-
+
Trypsin
-
+
-
+
VP40
Rab11

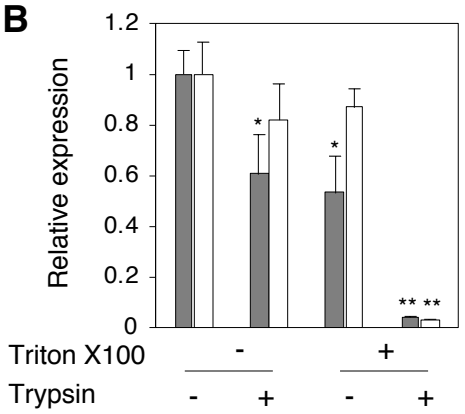
B
Relative expression
1.2
1
0.8
0.6
0.4
0.2
0
*
*
**
**
Triton X100
-
+
Trypsin
-
+
-
+

Fig.2

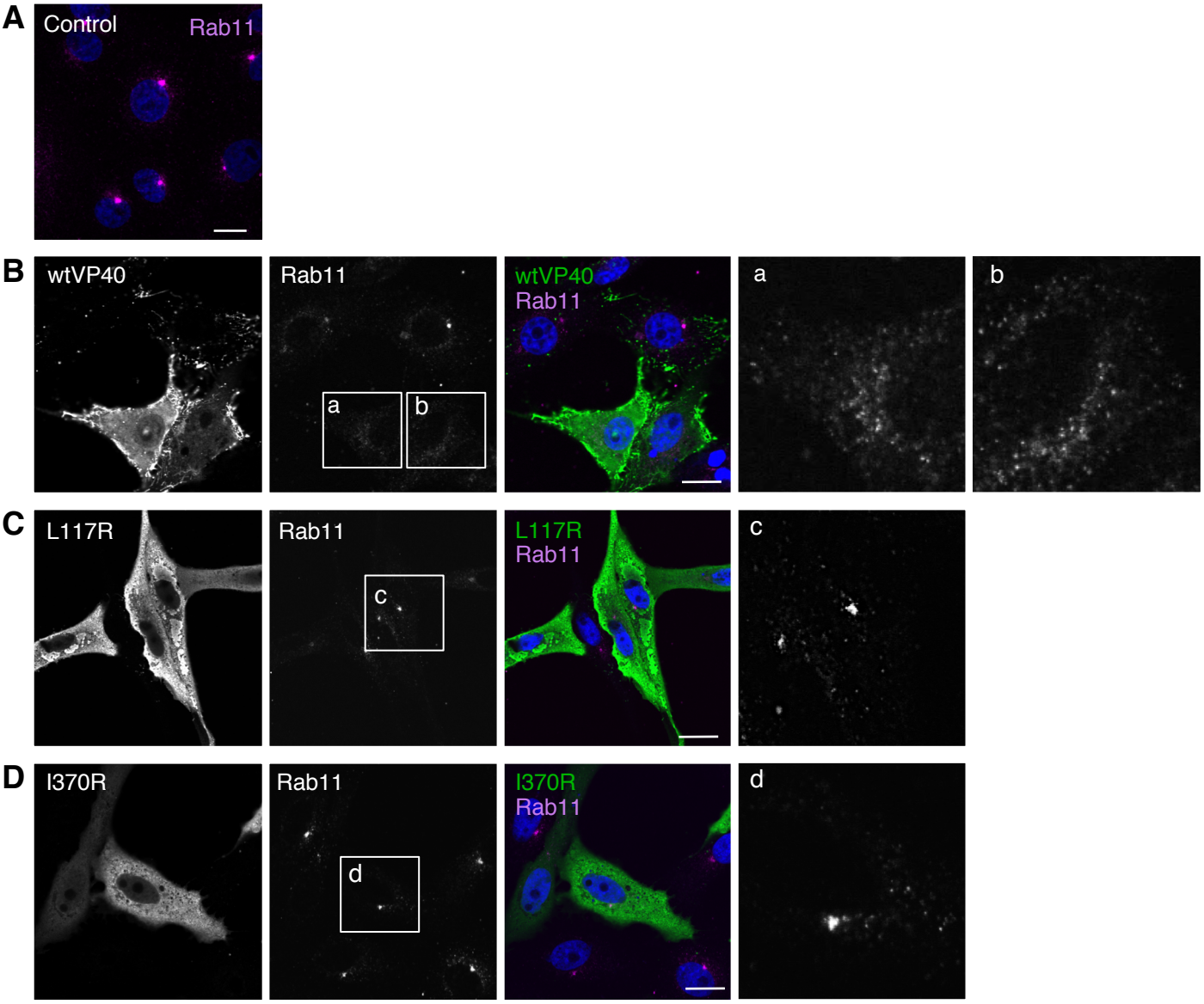
A
Control
Rab11
B
wtVP40
Rab11
a
b
wtVP40
Rab11
a
b
C
L117R
Rab11
c
L117R
Rab11
c
D
I370R
Rab11
d
I370R
Rab11
d

Fig.3

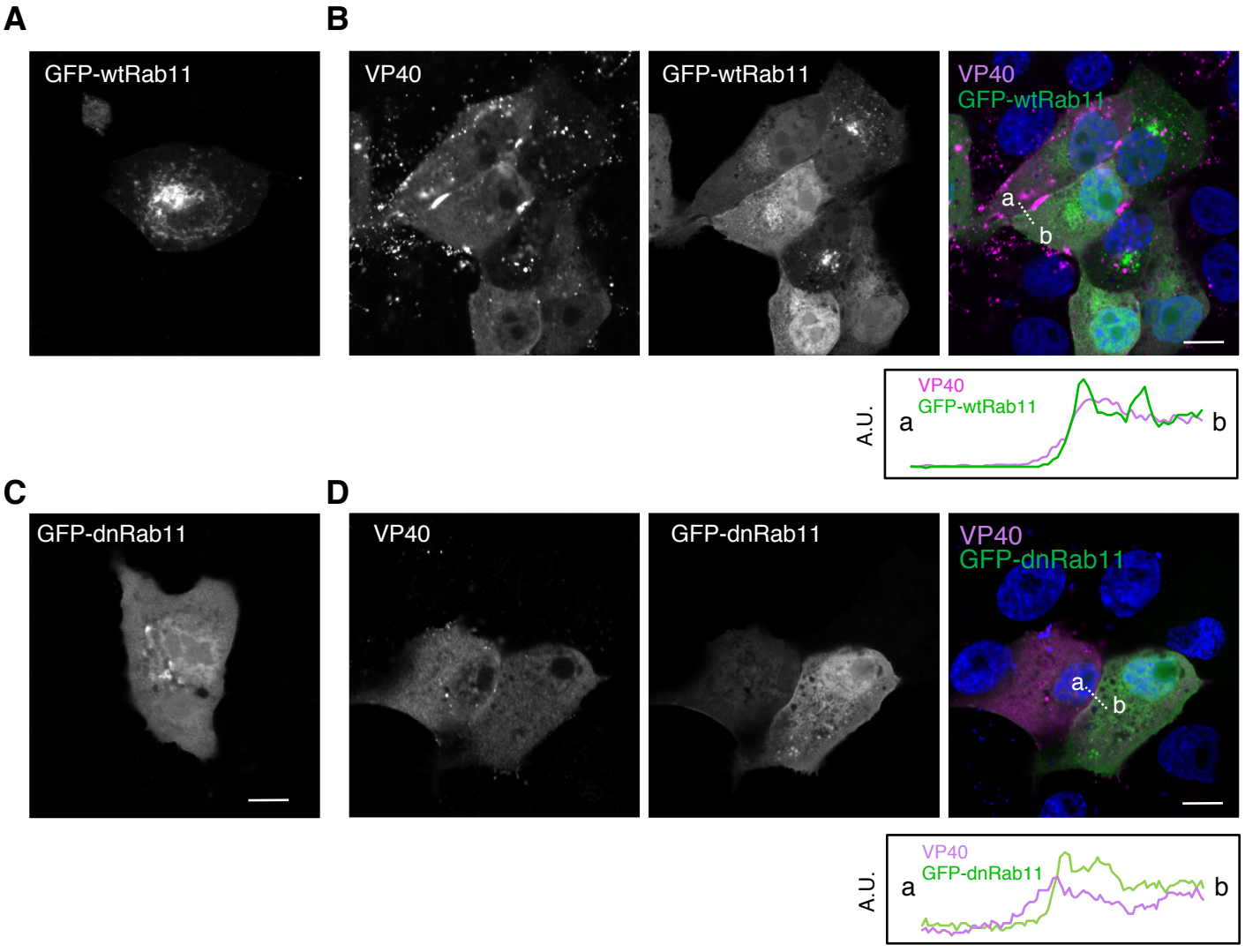
A
GFP-wtRab11
B
VP40
GFP-wtRab11
VP40
GFP-wtRab11
a
b
A.U.
VP40
GFP-wtRab11
a
b
C
GFP-dnRab11
D
VP40
GFP-dnRab11
VP40
GFP-dnRab11
a
b
A.U.
VP40
GFP-dnRab11
a
b

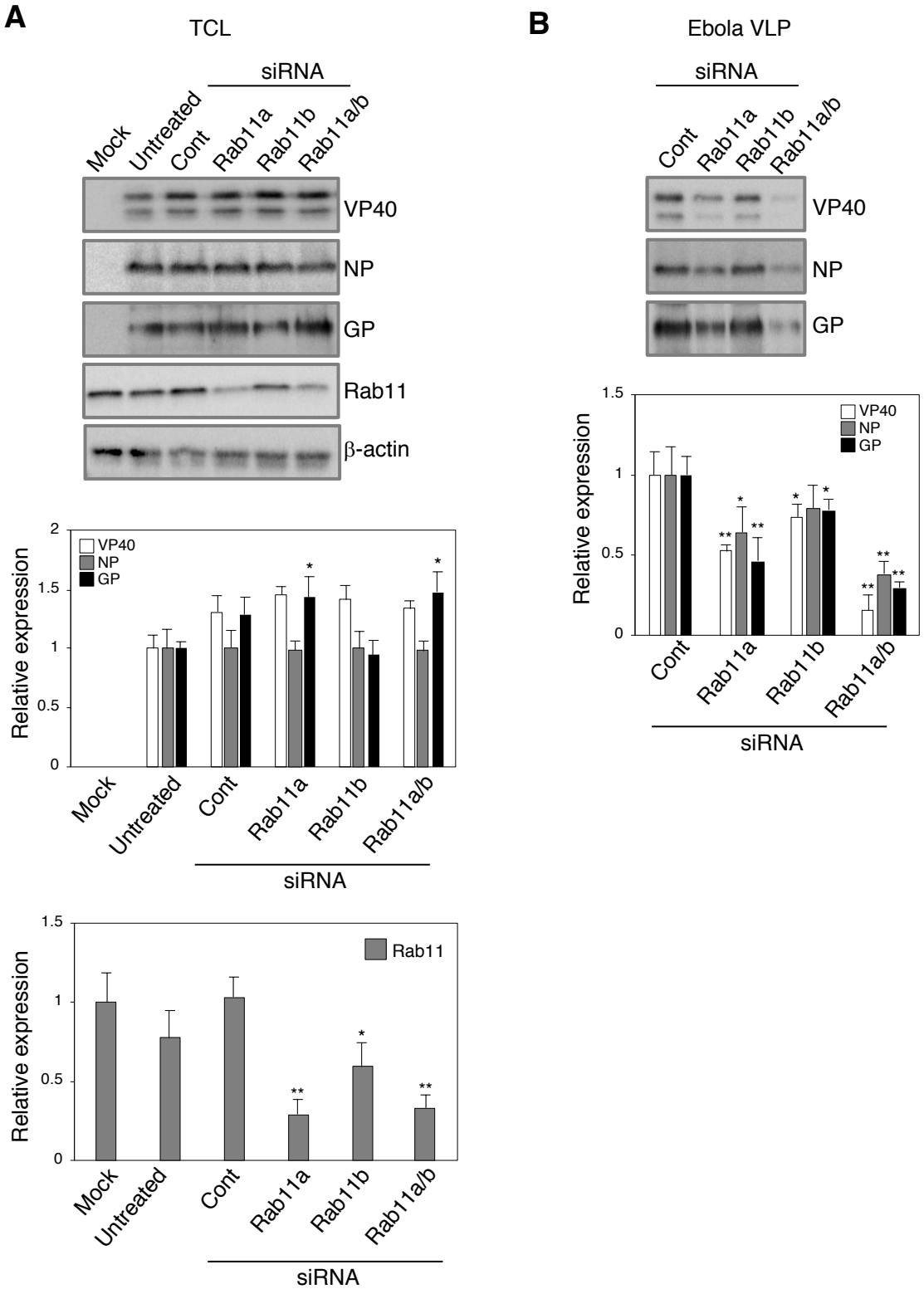
A
TCL
siRNA
Mock
Untreated
Cont
Rab11a
Rab11b
Rab11a/b
VP40
NP
GP
Rab11
β-actin
Relative expression
VP40
NP
GP
siRNA
B
Ebola VLP
siRNA
Cont
Rab11a
Rab11b
Rab11a/b
VP40
NP
GP
Relative expression
siRNA

Fig.5

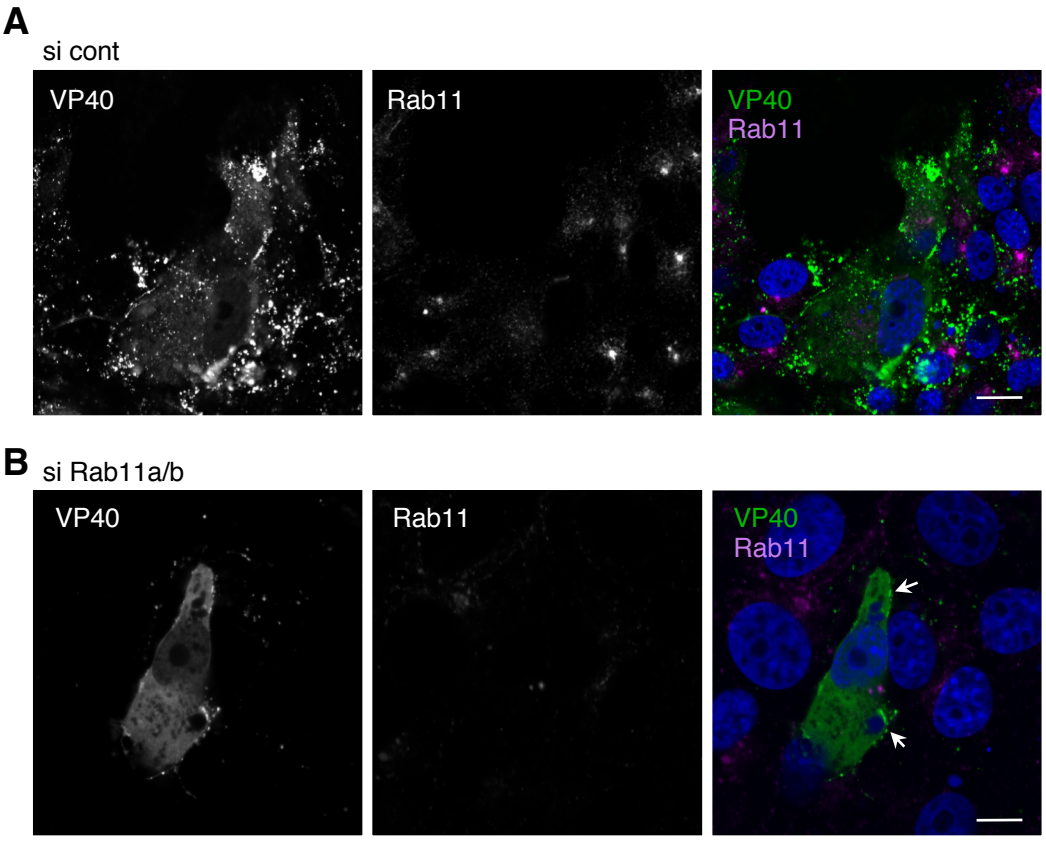
A
si cont
VP40
Rab11
VP40
Rab11
B
si Rab11a/b
VP40
Rab11
VP40
Rab11